Dalton Transactions

31P NMR Study of the Activated Radioprotection Mechanism of Octylphenyl-N,N-diisobutylcarbamoylmethyl Phosphine Oxide (CMPO) and Analogues

Journal:	*Dalton Transactions*
Manuscript ID	DT-ART-05-2019-001950.R1
Article Type:	Paper
Date Submitted by the Author:	14-Jun-2019
Complete List of Authors:	Horne, Gregory; Idaho National Laboratory, Center for Radiation Chemistry Research Kiddle, James; Western Michigan University, Chemistry Zarzana, Christopher; Idaho National Laboratory, Rae, Cathy; Idaho National Laboratory, Peller, Julie; Valparaiso University College of Arts and Sciences, Chemistry Cook, Andrew; Brookhaven National Laboratory, Chemistry Department Mezyk, Stephen; California State University at Long Beach, Chemistry and Biochemistry Mincher, Bruce; Idaho National Laboratory, Aqueous Separations and Radiochemistry

ARTICLE

^{31}P NMR Study of the Activated Radioprotection Mechanism of Octylphenyl-*N,N*-diisobutylcarbamoylmethyl Phosphine Oxide (CMPO) and Analogues

Received 00th May 2019,
Accepted 00th May 2019

DOI: 10.1039/x0xx00000x

Gregory P. Horne,*[a] James J. Kiddle,[b] Christopher A. Zarzana,[a] Cathy Rae,[a] Julie R. Peller,[c] Andrew R. Cook,[d] Stephen P. Mezyk,[e] and Bruce J. Mincher.[a]

We report a ^{31}P NMR investigation into the activated radioprotection mechanism of octylphenyl-*N,N*-diisobutyl-carbamoylmethyl phosphine oxide (CMPO) and analogues in the presence of a gamma radiation field. CMPO exhibits significantly enhanced radiation resistance in the presence of high nitric acid concentrations, compared to other ligands proposed for recovery of the trivalent actinides from spent nuclear fuel. The fundamental mechanism behind this activated radioprotection has been investigated using ^{31}P NMR and other supporting analytical techniques (GCMS and LCMS) in conjunction with systematic gamma irradiation studies, covering solvent system formulation and structural effects through the use of the CMPO analogues, dioctylphenylphospine oxide (DOPPO) and trioctylphosphine oxide (TOPO). These experiments have demonstrated that the acid-dependent, radioprotection mechanism requires a protonated phenyl-phosphine oxide motif to activate. Further, contacting these three ligand loaded organic phases with a range of mineral acids (nitric, sulfuric, hydrochloric, and perchloric acids) shows specificity for nitric acid (HNO_3), and the formation of a distinct [ligand•HNO_3] complex for CMPO and DOPPO, as identified by ^{31}P NMR, and predicted by DFT calculations. We propose that this complex is capable of sequential *n*-dodecane excited state quenching through the conjugated aromatic functionalities on the constituent CMPO and DOPPO molecules.

Introduction

The absorption of ionizing radiation by matter typically promotes ionization and electronic excitation followed by a cascade of chemical events, ultimately changing the chemical identity of the absorbing species and its surrounding environment. There are a number of chemical species that demonstrate enhanced stability and/or radioprotection mechanisms, rendering them more resistant to degradation, however, these mechanisms are not fully understood. Understanding radiation resistance aids in the design and development of chemical systems and materials for utility in medicine, space exploration, and the nuclear industry.

The bidentate Lewis base octylphenyl-*N,N*-diisobutylcarbamoylmethyl phosphine oxide (CMPO) (Figure 1, A) is one such apparent radiation resistant species. This compound was originally designed at Argonne National Laboratory as an extractant for trivalent actinides in the TRansUranium EXtraction (TRUEX) solvent extraction process.[1] CMPO has received considerable attention due to its unique radiolytic behaviour in conjunction to possessing structural moieties present in nature, e.g., the amidic (amino acids) and phosphoryl (ATP and DNA backbone) functionalities.

In the presence of a gamma (γ-) radiation field, the rate of radiolytic CMPO degradation in aerated *n*-dodecane solutions was found to significantly decrease upon contact with aqueous nitric acid (HNO_3), essentially becoming completely radiation-resistant at HNO_3 concentrations in excess of 5.0 M.[2] Under these highly acidic conditions, this corresponds to a radiolytic yield, *G*-value, of $G < 0.02$ μmol J^{-1}.[2] These results are consistent with earlier reports of chloroform solutions of tetraphenylmethylenediphosphine dioxide (Figure 1, D) contacted with 3-5 M HNO_3, which was found to exhibit an unusually high resistance to alpha (α-) and γ-irradiation during the extraction of trivalent americium and curium, following contact with HNO_3.[3] In the case of CMPO, the 'activated' radioprotection mechanism has been attributed to the formation of a sacrificial 1:1 [CMPO•HNO_3] complex in *n*-dodecane, as shown by equation (**1**):[2,4,5]

$$\text{CMPO} + HNO_3 \rightleftharpoons [\text{CMPO}\bullet HNO_3] \qquad K = 0.15. \qquad (\mathbf{1})$$

Once formed, [CMPO•HNO_3] allows for CMPO to be preserved at the expense of HNO_3. Under the biphasic solvent system conditions in which CMPO was designed to function – aerated

[a] *Idaho National Laboratory, Center for Radiation Chemistry Research, Idaho Falls, ID, P.O. Box 1625, 83415, USA*
[b] *Western Michigan University, Department of Chemistry, Kalamazoo, MI, 49008, USA.*
[c] *Valparaiso University, Department of Chemistry, Valparaiso, IN, 46383-6493, USA.*
[d] *Brookhaven National Laboratory, Department of Chemistry, Upton, NY , 11973, USA.*
[e] *California State University Long Beach, Department of Chemistry and Biochemistry, Long Beach, CA 90804, USA.*
**E-mail: gregory.p.horne@inl.gov*
† Electronic Supplementary Information (ESI) available: NMR data for all investigated systems. See DOI: 10.1039/x0xx00000x

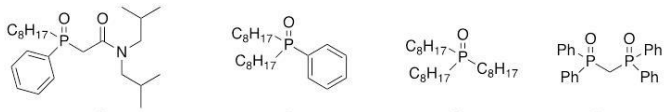

Figure 1. Chemical structures of octylphenyl-N,N-diisobutylcarbamoylmethyl phosphine oxide (CMPO, **A**), dioctylphenylphospine oxide (DOPPO, **B**), trioctylphosphine oxide (TOPO, **C**), and tetraphenylmethylenediphosphine dioxide (**D**).

alkane diluent in contact with concentrated aqueous HNO_3 – radiolysis promotes the formation of a plethora of decomposition products:[6]

$$R \rightsquigarrow e^-, H^\bullet, R^*, R^{\bullet+}, R^\bullet \quad (\mathbf{2})$$

$$H_2O \rightsquigarrow e^-, H^\bullet, {}^\bullet OH, H_2O_2, H_2, H_{aq}^+ \quad (\mathbf{3})$$

$$HNO_3 \rightsquigarrow e^-, {}^\bullet NO_3, HNO_2, O^\bullet, H_{aq}^+, \quad (\mathbf{4})$$

where R in the context of this work is *n*-dodecane. A number of these species are highly reactive and have been attributed to the cause of CMPO degradation, notably the ionized electron (e^-), *n*-dodecane radical cation ($R^{\bullet+}$), and hydroxyl ($^\bullet OH$) and nitrate ($^\bullet NO_3$) radicals:[7,8]

$$CMPO + e^- \rightarrow CMPO^{\bullet-} \quad (\mathbf{5})$$

$$CMPO + R^{\bullet+} \rightarrow CMPO^{\bullet+} + R \quad (\mathbf{6})$$

$$CMPO + {}^\bullet OH \rightarrow CMPO^\bullet + H_2O \quad (\mathbf{7})$$

$$CMPO + {}^\bullet NO_3 \rightarrow CMPO^\bullet + HNO_3. \quad (\mathbf{8})$$

The radiolytic impact of some of these species on CMPO is believed to be inhibited by a [CMPO•HNO_3] complex, as postulated for $R^{\bullet+}$:[7]

$$[CMPO{\bullet}HNO_3] + R^{\bullet+} \rightarrow CMPO + HNO_3^{\bullet+} + R. \quad (\mathbf{9})$$

Corresponding air-sparged steady-state γ-irradiation experiments yielded reduced rates of CMPO degradation, with no loss of CMPO in biphasic systems contacted with HNO_3 for concentrations as low as 2.0 M.[2] By continuously replenishing the concentration of dissolved O_2 in the organic phase (typical O_2 solubilities in aliphatic hydrocarbon correspond to 1-10 mM.)[9] the scavenging capacity ($k_s = k \times$ [scavenger]) for the reaction of O_2 with e^- and organic radicals ($R^\bullet$) was maintained, thereby inhibiting their contribution to CMPO degradation.[10,11]

$$O_2 + e^- \rightarrow O_2 \quad (\mathbf{10})$$

$$O_2 + R^\bullet \rightarrow RO_2^\bullet \quad (\mathbf{11})$$

$$RO_2^\bullet + RO_2^\bullet \rightarrow R{-}O{-}O{-}O{-}O{-}R \quad (\mathbf{12})$$

$$R{-}O{-}O{-}O{-}O{-}R \rightarrow \text{Products}. \quad (\mathbf{13})$$

Further, complimentary high linear energy transfer (LET) α-radiolysis experiments were performed by Mincher *et al.*[12] For the various α-radiation sources and solvent system conditions, they reported negligible ($G \leq 0.06$ μmol J^{-1}) CMPO degradation up to absorbed doses of 550 kGy. This implies that CMPO degradation is primarily instigated by radiolytic radical species, the yields of which are significantly reduced upon increasing LET, e.g., in going from γ-rays (^{60}Co 0.27 eV nm^{-1})[13] to α-particles (typically 100s of eV nm^{-1})[14]. This is further supported by experiments in which CMPO/*n*-dodecane solutions were spiked with 1 to 10 mM hydrogen peroxide (H_2O_2), a key oxidizing water radiolysis product whose radiolytic yield increases with LET: $G_\gamma = 0.07$, $G_\alpha = 0.17$ μmol J^{-1} in water at pH 7.[10,15,16] There was no observable change in the concentration of CMPO despite lengthy H_2O_2 exposure times.[12]

However, there are a number of discrepancies with the current interpretation of CMPO's radioprotection mechanism. Firstly, assuming the aforementioned sacrificial-protective mechanism, electrophilic attack on the proposed [CMPO•HNO_3] complex would yield $HNO_3^{\bullet+}$, which is synonymous with $^\bullet NO_3$ (E^0 = 2.3-2.6 V).[17] This radical should rapidly react with the now free CMPO ($k = 1 - 4 \times 10^8$ M^{-1} s^{-1})[8], thereby affording no net protection. Secondly, preservation of CMPO by maintaining dissolved O_2 concentration cannot be completely explained by its scavenging of e^-.[2] This is because nitrate (NO_3^-) is also an effective scavenger of e^-, and nitrate would be extracted into the organic phase as neutral HNO_3:

$$NO_3^- + e_{pre}^- \rightarrow NO_3^{\bullet 2-} \quad k = 1 \times 10^{13}\ M^{-1}\,s^{-1} \text{ in } H_2O \quad (\mathbf{14})$$

$$NO_3^- + e_{aq}^- \rightarrow NO_3^{\bullet 2-} \quad k = 9.7 \times 10^9\ M^{-1}\,s^{-1} \text{ in } H_2O. \quad (\mathbf{15})$$

Despite this, no difference in the rate of CMPO degradation was observed between irradiating organic-only and biphasic systems in contact with 0.1 M HNO_3.[2,12] This may be explained by the dependency of HNO_3 extraction by CMPO into the organic phase. Spencer *et al.* found that an assumed 1:1 CMPO:HNO_3 extraction stoichiometry was sufficient to interpret their data, to determine that approximately 4 mM HNO_3 is extracted by ≤0.2 M CMPO into *n*-dodecane contacted with 0.1 M HNO_3 at room temperature, and approximately 0.18 M was extracted when contacted with 3.0 M HNO_3 at 50 °C.[5] Thus, it could be argued that when CMPO/*n*-dodecane is contacted with 0.1 M HNO_3, insufficient HNO_3 is extracted into the organic phase to compete for e^-. However, Enomoto *et al.* found little difference in the decay rate for the triplet excited state of pyridine in liquid pyridine saturated with nitrous oxide (N_2O), another effective scavenger of electrons:[10,18]

$$N_2O + e^- \rightarrow N_2 + O^{\bullet-} \quad k = 9.1 \times 10^9\ M^{-1}\,s^{-1} \text{ in } H_2O, \quad (\mathbf{16})$$

whereas saturation with O_2 (~4.9 mM at 1 atm and room temperature in pyridine)[19] afforded a significant increase in the rate of triplet excited state decay. The significance of this observation is that O_2 is renowned for scavenging e^-, $R^\bullet$, and quenching excited states. Consequently, it could be argued that while O_2 is unable to compete for e^- versus recombination in *n*-dodecane[20], radioprotection of CMPO in the presence of O_2 maybe occurs through quenching *n*-dodecane excited-states (R^*):

$$O_2 + R^* \rightarrow O_2^* + R. \quad (\mathbf{17})$$

This implies that a fraction of CMPO degradation is induced by R^*.

Finally, it remains uncertain as to how the aforementioned observations relate to the activated radioprotection effect seen for CMPO. Despite extensive investigations into the radiolytic behaviour of CMPO containing solutions and solvent systems[2,12,21-24], little attention has been devoted to explaining the activated radioprotection mechanism, with our current

understanding limited to the postulated [CMPO•HNO_3] complex.

Here we present a systematic investigation into the nature of CMPO's radioprotection mechanism, by using ^{31}P NMR and a range of supporting analytical techniques in conjunction with an extensive suite of γ-irradiations, to probe the effect of solvent system formulation and structural effects on the radiolytic stability of CMPO and two of its analogues, (dioctylphenylphospine oxide (DOPPO, Figure 1 B) and trioctylphosphine oxide (TOPO, Figure 1 C). These analogues were chosen to provide a simple system to test the hypothesis that the radioprotection mechanism was due to the presence of a conjugated phenyl-phosphine oxide system.

Methods

Materials

CMPO (≥98%) and DOPPO (≥98%) were supplied by Eichrom (Lisle, IL, USA) and Avonyx Labs (Edison, NJ, USA), respectively. TOPO (99%), nitric acid (HNO_3, ≥99.999% trace metals basis), deuterated nitric acid (d-HNO_3, 65 wt. % in D_2O, 99 atom % D), perchloric acid ($HClO_4$, ACS reagent grade), deuterated octane (octane-d18, 98 atom % D), and *n*-dodecane (≥99% anhydrous) were obtained from Sigma Aldrich (St. Louis, MO, USA). Sulfuric acid (H_2SO_4, purissa grade) from Fluka (Honeywell, Charlotte, NC, USA), and hydrochloric acid (HCl, reagent grade) was supplied by BDH (VWR, Radnor, PA, USA). Unless otherwise specified, all solvents for analyses were Fisher (Hampton, NH, USA) Optima LC/MS grade. All chemicals were used without further purification. Ultra-pure water (18.2 MΩ cm^{-1}) was used for all aqueous solutions.

Irradiations

Steady-state gamma irradiations were performed using a Shepherd 109-68R Cobalt-60 Irradiator Unit at The University of Notre Dame Radiation Laboratory. Samples consisted of either neat *n*-dodecane solutions (organic-only) or biphasic solvent systems contacted with an equivalent volume of aqueous mineral acid solution. Contacted samples were agitated overnight prior to irradiation. Samples, comprising of 0.5 or 1.0 mL of each phase, were irradiated in 0.5 or 1 dram screw-cap glass vials to gamma doses ranging from 50 to 600 kGy. Dosimetry was performed using Fricke solution[25], and corrected for the radioactive decay of cobalt-60 ($\tau^1/_2$ = 5.27 years) affording an average dose rate of 1.85 Gy s^{-1}. Absorbed doses were calculated by correcting for the electron density of *n*-dodecane, 0.78.

Analytical Procedure

^{31}P NMR Analysis. A Bruker (Billerica, MA, USA) Avance 400 MHz spectrometer was used to perform proton-decoupled ^{31}P NMR using 85% H_3PO_4 as an external reference solvent and 10% octane-d_{18} as an internal lock standard. Samples were prepared by placing 0.45 mL of the ligand/*n*-dodecane/octane-d_{18} irradiated solution in an NMR tube and acquiring 128-scans per spectra. Complete spectra are reported in ppm and given in *Supplementary Information* (*SI*).

Ligand Quantification. The amount of each respective ligand (CMPO, DOPPO, and TOPO) was quantified using a combination of liquid chromatography mass spectrometry (LCMS), and gas chromatography with flame ionization detection (GC-FID):

- *LCMS.* Liquid chromatographic separations were performed with a Waters™ (Milford, MA, USA) Acquity UPLC H-class system equipped with a BEH C8 column (1.7 µm) and a QDa detector. An isocratic flow of 60% aqueous (0.1% formic acid) and 40% organic (2-propanol with 3.6% octanol) was employed.[16] The solvent flow rate was 0.15 mL min^{-1}, with the column and sample compartment temperatures held constant at 50 and 40 °C, respectively. The mass spectrometer was utilized in the positive scan mode and a cone voltage of 15 V.
- *GC-FID*. An Agilent (Santa Clara, CA, USA) 7890 Series II and a Hewlett Packard 6890 gas chromatograph were employed for gas chromatographic analysis. Separation was achieved using a Restek (Bellefonte, PA, USA) Rtx-5 30m x 0.25mm ID x 0.25µm df column. The Flame Ionization Detector (FID) temperature and gas chromatograph injector temperature were held at 300 °C with a split ratio of 15:1. The gas chromatograph oven was held at 100 °C for 1 min, ramped at 15 °C min^{-1} to 300 °C, and finally held at 300 °C for 2 min. Received samples were diluted 1:50 in 2-propanol prior to injection, and each sample was injected 4 times. Quantification of each compound was accomplished using 7-point calibration curves prepared from neat material, from 0 (process blank) to 7 mM for each analyte. For all three analytes, each calibration standard was injected 4 times. The sample injection order was randomized, and continuing calibration check standards at 3, 4, and 6 mM were injected in the middle and at the end of the runs to ensure the validity of the calibration curve.

Density Functional Theory

Calculations were performed using the Gaussian16 and Gaussview programs.[26] Geometries and energies were computed with the B3LYP functional and the 6-31G(d) basis set, and used the polarizable continuum *n*-dodecane solvent model. Frequency calculations were used to ensure stable geometries and not saddle points, and provide free energies.

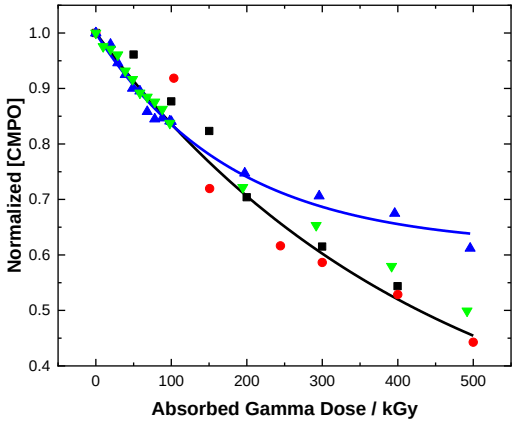

Figure 2. Gamma radiolysis of 50 mM CMPO/*n*-dodecane as a function of absorbed gamma dose: organic-only (■), biphasic contacted with 0.1 (●) or 3.0 M (▲) aqueous HNO_3, and phase separated pre-contacted with 3.0 M aqueous HNO_3 (▼). First-order decay fitted curves to only guide the eye.

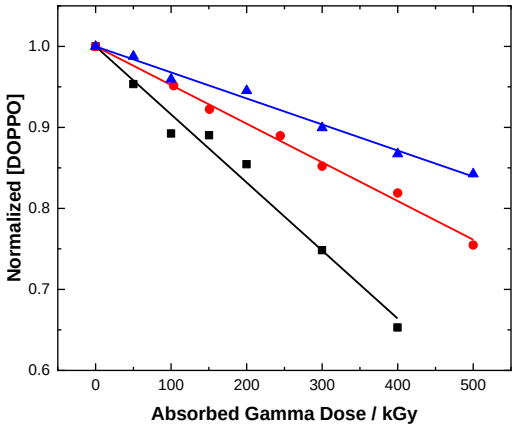

Figure 3. Gamma radiolysis of 50 mM DOPPO/*n*-dodecane as a function of absorbed gamma dose: organic-only (■), and biphasic contacted with 0.1 (●) or 3.0 M (▲) aqueous HNO_3. Linear fitted lines to only guide the eye.

Results and Discussion

Degradation Rates

The radiolytic degradation of CMPO, DOPPO, and TOPO in *n*-dodecane organic-only solutions or contacted biphasic solvent systems are given in Figures 2, 3, and 4, respectively. Concentrations have been normalized for comparison, a consequence of up to 30% loss in CMPO signal for HNO_3 concentrations ≥2.0 M.[21] This signal intensity 'loss' has also been attributed to the formation of the [CMPO•HNO_3] complex.[21] All three compounds were susceptible to γ-radiolysis, showing continued degradation as a function of absorbed dose. However, the rate of ligand degradation and extent of radioprotection are seen to be structurally dependent, as indicated by their respective dose constants summarized in Table 1.[27] Note that under our irradiation conditions the majority of radiolytic degradation is predominantly through indirect effects, as the energy deposited by ionizing radiation is partitioned between the constituents of the medium being traversed, proportional to their contribution to the total electron density of the medium, i.e., their electron fraction.[28] Consequently, all three compounds receive less than 5% of their total energy from direct deposition.

Table 1. Pseudo-first-order decay constants for the gamma irradiation of CMPO, DOPPO, and TOPO in *n*-dodecane as a function of solvent system formulation.

Ligand	Electron Fraction (%)	Decay Constant ($\times 10^{-6}$ Gy^{-1})		
		Organic-Only	0.1 M HNO_3	3.0 M HNO_3
CMPO	4.8	1.67 ± 0.07	1.65 ± 0.16	mixed-order 1.11 ± 0.07 to 0.77 ± 0.12
DOPPO	4.3	1.03 ± 0.08	0.61 ± 0.04	0.34 ± 0.02
TOPO	4.8	0.69 ± 0.06	0.57 ± 0.03	0.69 ± 0.04

For all of the CMPO solvent system permutations given in Figure 2, the initial (0 to ~200 kGy) rate of radiolytic degradation is relatively insensitive to the concentration of contacted HNO_3. An initial average dose constant of 1.67×10^{-6} Gy^{-1} was found, in agreement with non-contacted organic-only values reported by Mincher *et al.*[2] For sufficiently high absorbed doses (>200 kGy) a radioprotective effect of ~60% is observed when the organic phase is contacted with 3.0 M HNO_3, effectively reducing the dose constant to 0.77×10^{-6} Gy^{-1}, which is consistent with previous reports.[2,12] This phenomena is constrained to the presented biphasic systems irradiated in contact with 3.0 M HNO_3. Irradiation of phase-separated, pre-contacted CMPO/*n*-dodecane solutions yielded negligible activated radioprotection. This suggests that the radioprotection mechanism for CMPO relies on sufficiently high contacted acid concentrations and an interfacial mass transfer

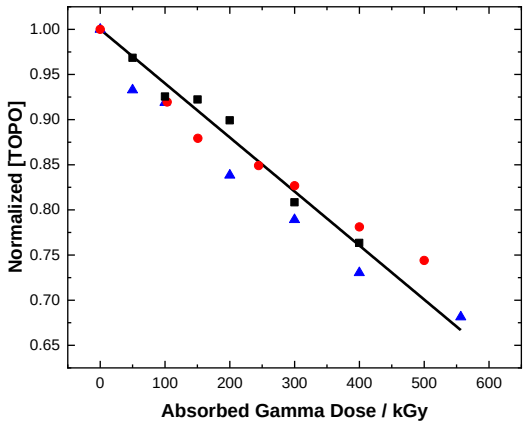

Figure 4. Gamma radiolysis of 50 mM TOPO/*n*-dodecane as a function of absorbed gamma dose: organic-only (■), and biphasic contacted with 0.1 (●) or 3.0 M (▲) aqueous HNO_3. Linear fitted line to only guide the eye.

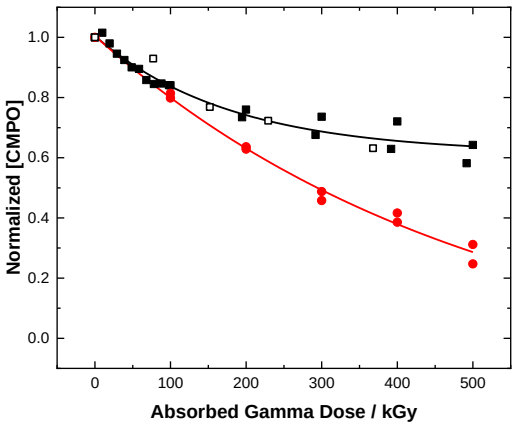

Figure 5. Gamma radiolysis of 50 mM CMPO/*n*-dodecane contacted with 3.0 M aqueous mineral acid as a function of absorbed gamma dose: (■) HNO_3, (□) HNO_3 from Elias *et al.*, and (●) H_2SO_4. First-order decay fitted curves to guide the eye.

process, possibly for replenishing the HNO_3 component of the complexed CMPO, [CMPO•HNO_3].

DOPPO demonstrates the most evident and systematic activated radioprotection effect, as shown in Figure 3. The extent of radioprotection increases with increasing HNO_3 concentration whilst maintaining a linear rate of degradation, attaining ~42% protection for 0.1 M (0.61×10^{-6} Gy^{-1}, $G = 0.47 \pm 0.01$ µmol J^{-1}), and ~67% protection for 3.0 M HNO_3 (0.34×10^{-6} Gy^{-1}, $G = 0.32 \pm 0.01$ µmol J^{-1}), relative to organic-only DOPPO/*n*-dodecane (1.03×10^{-6} Gy^{-1}, $G = 0.84 \pm 0.03$ µmol J^{-1}). These data suggest the formation of an analogous complex, [DOPPO•HNO_3].

TOPO is initially the most radiolytically stable of the three ligands, Figure 4. While P–C bonds are known to be strong, it is particularly curious that TOPO is more radiation resistant than CMPO and DOPPO, since the presence of an aromatic ring is typically synonymous with radiation resistance.[13] However, TOPO exhibits negligible activated radioprotection upon contacting with aqueous HNO_3, maintaining the same linear rate of decay, within experimental error, and affording an average dose constant of 0.65×10^{-6} Gy^{-1}, $G = 0.59 \pm 0.005$ µmol J^{-1}.

Comparison of these three ligands provides significant clues as to the mechanism by which activated radioprotection occurs in CMPO and DOPPO. It may be argued that radioprotection relies on the scavenging of detrimental *n*-dodecane radiolysis products by extracted aqueous HNO_3, for example, by inhibiting reactions (**5**) to (**7**). However, this cannot be the predominant means of radioprotection, because indirect radiolysis of HNO_3 generates problematic secondary products (e.g., $NO_3^{\bullet}$ and HNO_2) capable of propagating degradation.[8,29,30] Further, the extent of radioprotection is strongly dependent on the molecular structure of the investigated ligands, indicating an alternative radioprotection mechanism. CMPO is the least radiolytically stable of the three ligands, which may be explained by the additional amidic functionality, absent from both DOPPO and TOPPO. The radiolytic degradation products from amide containing ligands have been extensively studied and are characterized by facile cleavage of C–N bonds, liberating a variety of degradation products.[2,12,31-38] The absence of any acid activated radioprotection by TOPO indicates that an aromatic functionality is critical for this phenomenon, i.e., interaction with the phosphine oxide center alone is not sufficient to activate radioprotection. Finally, radioprotection is only activated upon contacting with an acidic aqueous phase. Thus, the activated radioprotective mechanism displayed by CMPO and DOPPO is an interaction between functionalities on the ligands and the extracted aqueous acidic phase, supporting the concept of a [ligand•HNO_3] complex.

Acid Contact Dependence

To ascertain the significance of the acidic aqueous phase, CMPO/*n*-dodecane solutions were irradiated in contact with different mineral acids, these data are given in Figure 5. Investigated mineral acids were selected on the basis of trying to understand whether acidity alone is sufficient to promote radioprotection or whether a combination of acidity and specific anion is required. Contacting with 3.0 M $HClO_4$ resulted in the immediate formation of an insoluble milky substance, assumed to be a degradation product of CMPO. Analysis of the resultant organic phase and subsequent irradiations showed that all of the CMPO had been destroyed by $HClO_4$ prior to irradiation.[39] Consequently, it was not possible to discern whether or not $HClO_4$ is capable of activating the radioprotection mechanism. Contacts with H_2SO_4 concentrations below 6.0 M avoided the formation of an insoluble polymeric substance. However, extracted H_2SO_4

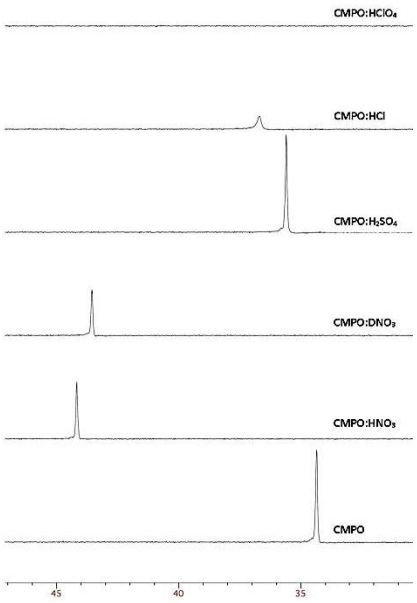

Figure 6. Section of the organic phase ^{31}P NMR spectra for formally 0.1 M CMPO/*n*-dodecane pre-equilibrated with 3.0 M aqueous acid (HNO_3, DNO_3, H_2SO_4, HCl, and $HClO_4$). Complete ^{31}P NMR spectra are given in *Figure S3* of *SI*.

clearly increased the rate of CMPO degradation upon irradiation, affording a dose constant of 2.59×10^{-6} Gy^{-1}. This suggests that H_2SO_4 does not form the same type of complex with CMPO as HNO_3, and instead enhances degradation through indirect radiolytic processes, for example, through formation of the sulphate radical ($SO_4^{\bullet-}$, E^0 = 2.5–3.1 V vs. NHE).[40,41]

Further interrogation of these contacted CMPO/*n*-dodecane systems was performed using ^{31}P NMR (Figure 6). Phosphorous NMR spectroscopy is highly informative about the phosphorous atoms' molecular environment (electronically and sterically), with most phosphorous-containing compounds having chemical shifts over a range of about 500 ppm in well-defined regions.[42] These characteristics of ^{31}P NMR spectroscopy make it uniquely suited to determine the structure of phosphorous containing compound(s) that are produced when CMPO is contacted with a mineral acid and subsequent γ-irradiation.[43]

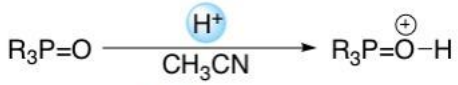

R	^{31}P δ	H^+	pK_a	^{31}P δ	ref.
Ph	25.0	H_2SO_4	-3.0	58.0	44
Et	6.3	CH_3SO_3H	-2.6	52.3	45

Figure 7. Protonation mechanism for triphenylphosphine oxide contacted with H_2SO_4.

Contacting CMPO/*n*-dodecane/octane-d_{18} with 3.0 M HNO_3 produces a quantitative downfield shift of the CMPO signal (^{31}P NMR, CMPO δ = 34.3 ppm; [CMPO•HNO_3] δ = 44.1 ppm), consistent with previous literature reports for the

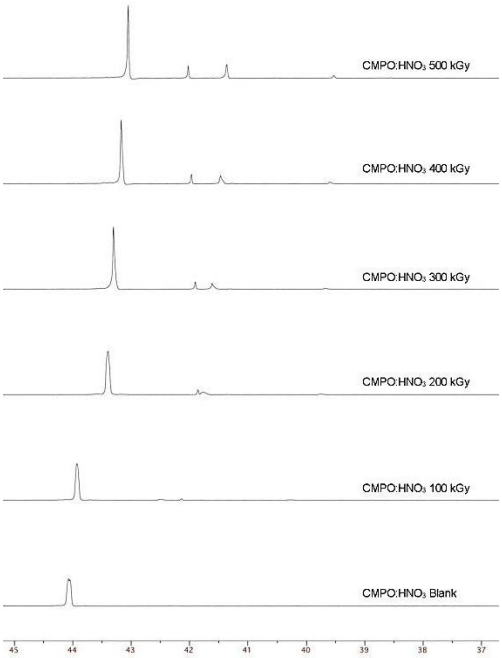

Figure 8. Section of organic phase ^{31}P NMR spectra for formally CMPO/*n*-dodecane contacted with 3.0 M HNO_3 as a function of absorbed gamma dose. Complete ^{31}P NMR spectra are given in *Figure S11* of *SI*.

quantification of the hydrogen bonding ability of triethyl and triphenylphosphine oxide with Lewis acids (Figure 7).[44,45] The downfield shift for the [CMPO•HNO_3] complex is indicative of protonation of the Lewis basic phosphoryl oxygen, causing a decrease in the π-bond character of the P=O bond, and an increased polarization of the σ-bond, resulting in deshielding of the phosphorous atom.[46,47] Complex formation is further supported by previous studies that showed a downfield shift for the ^{31}P NMR signal of CMPO when complexed with carboxylates.[48]

The presence of a sharp single resonance in the ^{31}P NMR (Figure 6) suggests the exclusive protonation of the phosphine oxide since the equilibrium with a hydrogen bonded complex would produce significant line broadening.[46] This interaction is supported by ^{31}P NMR data for $\Delta\delta$(CMPO) vs. [HNO_3] (*Supporting Information Figure S2 and S4*), where the HNO_3 concentration is increased while maintaining the CMPO concentration. The downfield shift of the ^{31}P NMR signal of CMPO is interpreted as an indication of the formation of a protonated phosphoryl oxygen atom.

Further evidence for the formation of a [CMPO•HNO_3] complex was obtained by its formation with 3.0 M deuterated nitric acid (DNO_3). The [CMPO•DNO_3] complex (δ = 43.6 ppm) shows an incremental up-field shift of the phosphorus signal, consistent with the Born-Oppenheimer approximation for replacement of ^{1}H with ^{2}H, that shows a dependence of atomic motion with mass increment that directly effects the ^{31}P shielding tensor.[49]

^{31}P NMR data from contact of CMPO with H_2SO_4 and HCl show similar, but smaller, downfield chemical shifts of 35.6 and

36.6 ppm, respectively (Figure 6). These smaller chemical shift changes can be attributed to differences in pK_a that has been shown to correlate with the chemical shift of phosphine oxide Lewis base complexes.[46] However, these data indicate that acid concentration, likely due to competition with complex formation with water molecules, has an impact on the acid-base reaction of CMPO in nonpolar media.[48]

In addition to characterizing the phosphorous species formed from initial contact with the four acids, ^{31}P NMR spectra of samples taken during the course of irradiation were obtained. Figure 8 shows the signals from phosphorus species produced as a function of dose from the γ-irradiation of the initially formed [CMPO•HNO_3] complex. There is a dose dependent formation of four different major organophosphorus species upon irradiation of the initial [CMPO•HNO_3] complex (δ = 42.0 ppm). Based on the up-field change in phosphorous chemical shift, these species are phosphine oxides similar in functionality to the [CMPO•HNO_3] complex, but distinctly different organophosphorous compounds, as based on the sensitivity of ^{31}P NMR chemical shifts to electronic and steric factors.[43] The gradual up-field shift of the dominant [CMPO•HNO_3] complex signal in Figure 8 with absorbed dose reflects changes in the solvent system's composition due to radiolysis, which in turn effects the phosphorus atom's environment and thus its chemical shift. Assuming a *G*-value for *n*-dodecane radiolysis of between 0.42 and 0.85 μmol J^{-1},[50,51] based on radical garment yields, a 500 kGy absorbed dose corresponds to the conversion of 0.21-0.43 M *n*-dodecane into radiolysis products. Of this amount, ~20 mM of these *n*-dodecane radiolysis products are involved in [CMPO•HNO_3] complex degradation (Figure 2), leaving 0.19-0.41 M to either undergo recombination or formation of steady-state *n*-dodecane degradation products. Therefore, under the experimental conditions reported here, there is sufficient radiation-induced modification of the *n*-dodecane solvent to influence chemical shift, as demonstrated by Figures S5–S8 in SI. The changes in chemical shift as a function of absorbed dose may be due to the formation of degradation products containing carbonyl functionalities, see the *Identification of CMPO Radiolytic Degradation Products using LC-MS* section in *SI*.

Overall, the ^{31}P NMR signals provide significant support for the formation of a [CMPO•HNO_3] complex (δ = 44.1 ppm) downfield from the initial CMPO signal (δ = 34.3 ppm), and that this behaviour is specific to HNO_3. Further evidence in support of these data are observations for similar variations in the ^{31}P NMR chemical shifts for DOPPO and TOPO (*Figures S7 – S12 in SI*): DOPPO (DOPPO, δ = 34.8 ppm; [DOPPO•HNO_3], δ = 45.9 ppm) and TOPO (TOPO, δ = 41.5 ppm; [TOPO•HNO_3], δ = 56.1 ppm) when contacted with 3.0 M HNO_3. Interestingly, TOPO forms an analogous protonated complex, [TOPO•HNO_3], highlighting the need for both protonation and an aromatic moiety to activate radioprotection.

Complex Geometry

Molecular structure computations support the formation of a stable neutral [CMPO•HNO_3] complex in *n*-dodecane, with respect to non-complexed CMPO and HNO_3, finding a free energy (ΔG) for complexation of -0.12 eV. Despite attempts to make HNO_3 more equally bridged across the CMPO carbonyl group, the most stable geometry finds the proton in HNO_3 preferentially favouring a hydrogen bond to the phosphoryl oxygen, with a distance of 1.57 Å, as shown in Figure 9. In the lowest energy structure, the distance to the carbonyl oxygen is 2.8 Å. This geometry is consistent with the ^{31}P NMR results. Further, the preference for HNO_3 to hydrogen bond to the phosphoryl oxygen functionality is reproduced by calculations for DOPPO. A similar complex is formed, [DOPPO•HNO_3] (*Figure S1 in Supplementary Information*), affording a hydrogen bond distance to the carbonyl oxygen of 1.55 Å, and a ΔG = -0.25 eV for reaction of HNO_3 with DOPPO in *n*-dodecane.

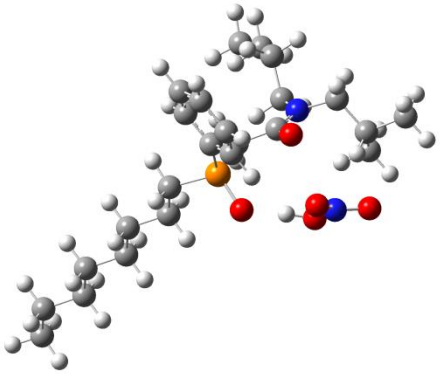

Figure 9. Molecular geometry for the [CMPO•HNO_3] complex calculated using the B3LYP functional and the 6-31G(d) basis set. Phosphorous atoms are shown in orange, oxygen in red, nitrogen in blue, carbon in grey, and hydrogen in off white.

Mechanism for Activated Radioprotection

The aromatic functionality of CMPO and DOPPO coupled with a sufficiently concentrated aqueous HNO_3 phase is key to the mechanism for activated radioprotection. Aromatic compounds are generally more stable to radiation than corresponding aliphatic compounds, and are able to impart this relative stability to other compounds through inter- and/or intramolecular interactions via physical (energy transfer/quenching) and chemical (scavenging) processes.[13] This is a consequence of their delocalized π-electron system disfavouring fragmentation and promoting efficient quenching of excited states.

We propose that the mechanism for activated radioprotection is through sequential quenching of *n*-dodecane excited states (R*) by the [ligand•HNO_3] complex:

$$\text{ligand} + R^* \rightarrow \text{ligand}^* + R \quad (\mathbf{18})$$

$$\text{ligand}^* \rightarrow \text{degradation products} \quad (\mathbf{19})$$

$$[\text{ligand}\bullet HNO_3] + R^* \rightarrow \text{ligand} + HNO_3^* + R. \quad (\mathbf{20})$$

Dodecane possess a relatively low dielectric constant (2.00),[52] affording rapid ion-recombination ($R^{\bullet+} + e^-$) within ~2 ns[20], populating a mixture of *n*-dodecane excited states. The lifetimes of these excited states has been reported as between 3 and 4 ns,[53] presenting sufficient time for scavenging by relatively high concentrations of CMPO/DOPPO, assuming a

diffusion limited quenching rate coefficient. Tabuse *et al*. found that the addition of small amounts (≤10 mM) of a variety of aromatic solutes to *n*-dodecane reduced the yield of scission products, and thus overall degradation.[51] By using nanosecond pulse radiolysis techniques, they were able to confirm the ability of these aromatic solutes to react with the initial radiolysis products from *n*-dodecane, i.e., R*, $R^{\bullet+}$, and e^-. All of the aromatic solutes reacted with R* and $R^{\bullet+}$, whereas non-conjugated aromatics were found not to react with e^-. This aromatic radioprotective effect was further characterized by LaVerne and Dowling-Medley, who demonstrated efficient inter- and intramolecular energy transfer from aliphatic to aromatic entities.[54] Of particular importance is their observation that despite the addition of progressively longer carbon chains to benzene, the radiolytic response of the molecule is more aligned with that of the aromatic component and not the aliphatic. This further highlights the efficiency of the aromatic intramolecular energy transfer mechanism, and the feasibility of CMPO/DOPPO to receive excitation energy and shuttle it to their aromatic component. Once localized on the aromatic functionality, a variety of excited state processes allow for energy dissipation and ultimately degradation of the molecule, yielding a mixture of hydrogen atoms, carbon centered radicals, unsaturated molecules, and molecular hydrogen.[55-60]

Previous CMPO degradation product analysis found no evidence for nitration or hydroxylation of the aromatic ring nor aliphatic side chains, which would be expected if electrophilic processes were predominantly responsible for its degradation.[12,61] Instead, a variety of degradation products originating from cleavage of C–C, C–N, and C–P bonds were measured, suggesting that excited state fragmentation processes play a significant role. This is in keeping with previous observations pertaining to continuous O_2 sparging – resulting in enhanced radiolytic stability through the quenching of excited states.[2] Further, HNO_3 has been shown to quench excited states in aqueous nitrate and nitric acid media.[62,63] This may provide some answer as to why the activated radioprotective mechanism is dependent upon HNO_3 complexation, and not the other investigated mineral acids. With this in mind, we can envision a mechanism by which the aromatic functionality of CMPO and DOPPO quenches R* and then shuttles that excitation energy to the nearby NO_3^- in [ligand•HNO_3], generating NO_3^-*. The fate of NO_3^-* can be expected to not be too dissimilar from the aqueous phase: >50% quenched to ground-state, and the remaining subject to partitioning between rearrangement to peroxynitrous acid (ONOOH) and fragmentation:[64]

$$ONOOH \rightarrow NO + O_2^- \text{ or } NO^- + O_2. \quad (21)$$

This also provides an explanation for the need for biphasic conditions to regenerate the [ligand•HNO_3] complex.

Conclusions

The activated radioprotection mechanism for CMPO/n-dodecane contacted with a range of nitric acid concentration has been investigated. Gamma irradiation of aerated n-dodecane solutions of CMPO, and the two analogues DOPPO and TOPO, demonstrates the critical need for a protonated phenyl-phosphine oxide functionality to activate this radioprotection mechanism. Further, contacting these organic phases with other mineral acids shows specificity for HNO_3, and the formation of a distinct [CMPO•HNO_3] complex, identified by ^{31}P NMR and predicted by DFT calculations. An argument has been presented for the mechanism of activated radioprotection for both CMPO and DOPPO, wherein we propose the formation of a 1:1 [Ligand•HNO_3] complex, capable of sequential *n*-dodecane excited state quenching through the conjugated aromatic functionalities on the constituent CMPO and DOPPO molecules.

Conflicts of interest

There are no conflicts to declare.

Acknowledgements

This research has been funded by the US-DOE Assistant Secretary for NE, under the FCR&D Radiation Chemistry program; DOE-Idaho Operations Office Contract DE-AC07-05ID14517 and Nuclear Energy Universities Program (NEUP) DE-NE0008406 grant. The gamma irradiations reported herein were performed at the Notre Dame Radiation Laboratory (NDRL). The NDRL is supported by the Division of Chemical Sciences, Geosciences and Biosciences, Basic Energy Sciences, Office of Science, United States Department of Energy (DOE) through Award No. DE-FC02-04ER15533. Electronic structure computations were carried out at Brookhaven National Laboratory supported by the Department of Energy, Office of Science, Office of Basic Energy Sciences, Chemical Sciences, Geosciences and Biosciences Division, under Contract No. DE-SC0012704 with the U.S. Department of Energy.

Notes and references

(1) E. P. Horwitz and D. G. Kalina, *Solv. Extr. Ion Exch.*, 1984, **2**, 179.

(2) B. J. Mincher, S. P. Mezyk, G. Elias, G. S. Groenewold, C. L. Riddle, and L. G. Olson, *Solv. Extr. Ion Exch.*, 2013, **31**, 715.

(3) N. E. Kochetkova, M. K. Chmutova, I. A. Lebedev, and B. F. Myasoedov, *RadioKhimiya*, 1981, **23**, 420

(4) T. Fuji, K. Aoki, and H. Yamana, *Sol. Extr. Ion Exch.*, 2006, **24**, 347.

(5) B. B. Spencer, R. M. Counce, and B. Z. Egan, *Environ. Energy Eng.*, 1997, **43 (2)**, 555.

(6) B. J. Mincher and S. P..; Mezyk, *Radiochim. Acta.*, 2009, **97**, 519.

(7) S. P. Mezyk, B. J. Mincher, S. B. Dhiman, B. Layne, and J. W. Wishart, *J. Radioanal. Nucl. Chem.*, 2016, **307**, 2445.
(8) S. P. Mezyk, T. D. Cullen, K. A. Rickman, and B. J. Mincher, *Int. J. Chem. Kin.*, 2017, **49 (9)**, 635.
(9) S. J. Ashcroft and B. I. Mustafa, *J. Chem. Eng. Dat.*, 1997, **42 (6)**, 1244.
(10) G. V. Buxton, C. L. Greenstock, W. P. Helman, A. B. Ross, *J. Phys. Chem. Ref. Data*, 1988, **17**, 513.
(11) Z. B. Alfassi, The Chemistry of Free Radicals: Pyroxyl Radicals. Wiley: Chichester, West Sussex, England, 1997, ISBN: 978-0-471-97065-1.
(12) B. J. Mincher, S. P. Mezyk, G. Elias, G. S. Groenewold, J. A. LaVerne, M. Nilsson, J. Pearson, N. C. Schmitt, R. D. Tillotson, and L. G. Olson, *Solv. Extr. Ion Exch.*, 2014, **32**, 167.
(13) J. W. T. Spinks and R. J. Woods, An Introduction to Radiation Chemistry, 3rd ed.; 1991; John Wiley and Sons. Hobokken, NJ.
(14) J. F. Ziegler, J. P. Biersbak, and U. Littman, The Stopping and Range of Ions in Solids: 1985 Pergamon Press, New York, NY.
(15) M. LeFort and X. Tarrago, *J. Phys. Chem.*, 1959, ***63***, 833.
(16) O. Roth and J. A. LaVerne, *J. Phys. Chem. A*, 2011, ***115***, 700.
(17) P. -Y. Jiang, Y. Katsumura, K. Ishigure, and Y. Yoshida, *Inorg. Chem.*, 1992, **31**, 5135.
(18) K. Enomoto, J. A. LaVerne, S. Seki, and S. Tagawa, *J. Phys. Chem. A*, 2006, **110**, 9874.
(19) R. Battino, Oxygen and Ozone; Ed.; Solubility Data Series, Vol. 7; Pergamon Press: New York, 1981.
(20) Y. Yoshida, T. Ueda, T. Kobayashi, H. Shibata, and S. Tagawa, *Nucl. Inst. Meth. Phys. Res. A*, 1993, ***327***, 41.
(21) G. Elias, G. S. Groenewold, B. J. Mincher, and S. P. Mezyk, *J. Chroma. A*, 2012, **1243**, 47.
(22) N. Simonzadeh, A. M. Crabtree, L. E. Trevorrow, G. F. Vandegrift, Argonne National Laboratory Report ANL-90/14. July B1992B.
(23) M. V. Logunov, Yu. A. Voroshilov, N. P. Starovoitov, A. Yu. Shadrin, I. V. Smirnov, I. B. Kvasnitskii, I. G. Tananaev, B. F. Myasoedov, V. P. Morgalyuk, M. Kamiya, I. Koma, and T. Koyama, *Radiochemistry*, 2006, **48**, 55.
(24) R. Chiarizia and E. P. Horwitz, *Solvent Extra. Ion Exch.*, 1986, **4**, 677.
(25) R. Fricke and E. J. Hart, *J. Chem. Phys.*, 1935, **3**, 60.
(26) Gaussian 16, Revision A.03, M. J. Frisch, G. W. Trucks, H. B. Schlegel, G. E. Scuseria, M. A. Robb, J. R. Cheeseman, G. Scalmani, V. Barone, G. A. Petersson, H. Nakatsuji, X. Li, *et al.*, Gaussian, Inc., Wallingford CT, 2016.
(27) B. J. Mincher and R. D. Curry, *Applied Radiation and Isotopes*, 2000, **52 (2)**, 189.
(28) A. J. Swallow and M. Inokuti, *Radiat. Phys. Chem.*, 1988, **32**, 185.
(29) B. A. Moyer, Ion Exchange and Solvent Extraction a Series of Advances, Vol. 19; CRC Press: Boca Raton; 1990.
(30) B. J. Mincher, G. Modolo, and S. P. Mezyk, *Solv. Extr. Ion Exch.*, 2009, **27 (1)**, 1.
(31) K. L. Nash, R. C. Gatrone, G. A. Clark, P. G. Rickert, and E. P. Horwitz, *Sep. Sci. Technol.*, 1988, **23**, 1355.
(32) K. L. Nash, P. G. Rickert, and E. P. Horwitz, *Solv. Extr. Ion Exch.*, 1989, **7**, 655.
(33) J. N. Mathur, M. S. Murali, P. B. Ruikar, M. S. Nagar, A. T. Sipahimalani, A. K. Bauri, A. Banerji, *Sep. Sci. Technol.*, 1998, **33**, 2179.
(34) L. Berthon, J. M. Morel, N. Zorz, C. Nicol, H. Virelizier, and C. Madic, *Sep. Sci. Technol.*, 2001, **36**, 709.
(35) C. A. Zarzana, G. S. Groenewold, B. J. Mincher, S. P. Mezyk, A. Wilden, H. Schmidt, G. Modolo, J. F. Wishart, and A. R. Cook, *Solv. Extrac. Ion Exch.*, 2015, **33**, 431.
(36) H. Galan, C. A. Zarzana, A. Wilden, A. Nunez, H. Schmidt, R. J. M. Egberink, A. Leoncini, J. Cobos, W. Verboom, G. Modolo, G. S. Groenwold, and B. J. Mincher, *Dalton Trans.*, 2015, **44**, 18049.
(37) Y. Sugo, Y. Sasaki, and S. Tachimori, *Radiochim. Acta*, 2002, **90**, 161.
(38) B. J. Mincher, G. Modolo, and S. P. Mezyk, *Solv. Extr. Ion Exch.*, 2009, **27**, 579.
(39) R. Dalpozzo, R. Bartoli, L. Sambri, and P. Melchiorre, *Chem. Rev*. 2010, **110**, 3501.
(40) P. Neta, R. E. Huie, and A. B. Rosee, *J. Phys. Chem. Ref. Data*, 1988, **17**, 1027.
(41) L. Eberson, *Adv. Phys. Org. Chem.*, 1982, **18**, 79.
(42) J. C. Tebby, Handbook of Phosphorus-31 Nuclear Magnetic Resonance Data; CRC Press: Boca Raton, FL, 1991.
(43) L. D. Quin and J. G. Verkade, Phosphorus-31 NMR Spectral Properties in Compound Characterization and Structural Analysis; Wiley-VCH: Hoboken, NJ, 1994.
(44) K. M. Diemoz and A. K. Franz, *J. Org. Chem*., 2019, ***84***, 1126.
(45) K. B. Dillon, M. P. Nisbet, and T. C. Waddington, *J. Chem. Soc. Dalton Trans.*, 1982, 465.
(46) U. Mayer, V. Gutmann, and W. Gerger, *Monatsh. Chem*. 1975, **106**, 1235.
(47) V. Gutmann, *Coord. Chem. Rev*. 1976, **18**, 225.
(48) R. C. Gatrone and E. P. Horwitz, *Solv. Extr. Ion Exch*., 1987, **5**, 493.
(49) C. M. Lagier, D. C. Apperley, U. Scheler, A. C. Olivieri, and R. K. Harris, *J. Chem Soc. Faraday Trans.*, 1996, ***92***, 5047.
(50) L. Wojnarovits and R. H. Schuler, *J. Phys. Chem. A.*, 2000, **104**.
(51) S. Tabuse, Y. Izumi, T. Kojima, Y. Yoshida, T. Kozawa, M. Miki, S. Tagawa, *Rad. Phys. Chem.*, 2001, **62**, 179.
(52) C. Wohlfarth, Dielectric Constant of Dodecane. In Landolt-Börnstein - Group IV Physical Chemistry (Numerical Data and Functional Relationships in Science and Technology), vol 17. Springer, Berlin, Heidelberg, 2008.
(53) Y. Katsumura, Y. Yoshida, S. Tagawa, Y. Tabata, *Radiat. Phys. Chem.*, 1983, **21**, 103.
(54) J. A. LaVerne and J. Dowling-Medley, *J. Phys. Chem. A*, 2015, **119**, 10125.

(55) M. Rode, Aromatic Hydrocarbons. In Radiation Chemistry of Hydrocarbons. Elsevier: Amsterdam, 1981.
(56) E. A. Cherniak, F. S. Dainton, and E. L. Collinson, *Trans. Faraday Soc.*, 1964, **60**, 1408.
(57) J. A. LaVerne and M. S. Araos, *Rad. Phys. Chem.*, 1999, **55**, 525.
(58) R. A. Holroyd, Organic Liquids. In Fundamental Processes in Radiation Chemistry; Interscience: New York, 1968.
(59) A. Baidak, M. Badali, and J. A. LaVerne, *J. Phys. Chem. C*, 2011, **115**, 7418.
(60) J. A. LaVerne and A. Baidak, *Rad. Phys. Chem.*, 2012, **81**, 1287.
(61) G. S. Groenewold, G. Elias, B. J. Mincher, S. P. Mezyk, and J. A. LaVerne, *Talanta*, 2012, **99**, 909.
(62) G. P. Horne, S. M. Pimblott, and J. A. LaVerne, *J. Phys. Chem. B*, 2017, **121**, 5385.
(63) C. R. Gregson, G. P. Horne, R. M. Orr, S. M. Pimblott, H. E. Sims, R. J. Taylor, and K. J. Webb, *J. Phys. Chem. B*, 2018, **122 (9)**, 2627.
(64) D. Madsen, J. Larsen, S. K. Jensen, S. R. Keiding, and J. Thogersen, *J. Am. Chem. Soc.*, 2003, ***125***, 15571.

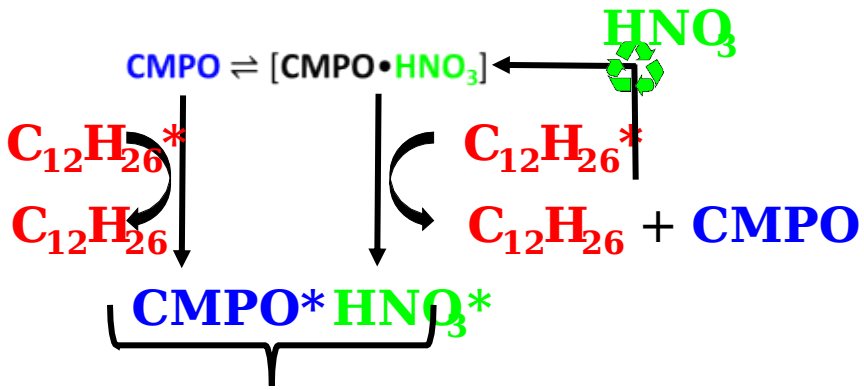

Quenching and Degradation